Available online at www.sciencedirect.com
ScienceDirect
Journal of Organometallic Chemistry 692 (2007) 1735–1747
Journal of Organometallic Chemistry
www.elsevier.com/locate/jorganchem

Dimethyltin(IV) complexes with zwitterionic buffers (Mes and Mops)

Mahmoud M.A. Mohamed [a,*], Elham M. Abd-Alla [b], Ahmed El-Sayed El-Badawy [c]

[a] Department of Sciences and Mathematics, New-Valley-Faculty of Education, Assuit University, Al-Kharga, New Valley, Egypt
[b] Department of Chemistry, Faculty of Science, Minia University, Minia, Egypt
[c] Medico-Legal Department of Forgery and Counterfeiting Research, Ministry of Justice, Egypt

Received 7 October 2006; received in revised form 24 December 2006; accepted 24 December 2006
Available online 9 January 2007

Abstract

Equilibrium studies in aqueous solution are reported for dimethyltin(IV) complexes of the zwitterionic buffers ''Good's buffer'', such as Mes and Mops (*L*). Stoichiometry and stability constants for the complexes formed were determined at different temperature and ionic strength 0.1 M $NaNO_3$. The results showed the best fit of the titration curves were obtained when complexes ML, MLH_{-1}, MLH_{-2}, and MLH_{-3} were expected beside the hydrolysis products of the dimethyltin(IV) cation. The thermodynamic parameters ΔH°, ΔS° and ΔG° calculated from the temperature dependence of the formation constant of the dimethyltin(IV)–Mes complex was investigated. The effect of dioxane as a solvent on the formation constants of dimethyltin(IV)–Mes complex was discussed. The concentration distribution of the various complex species was evaluated as a function of pH. The bonding sites of the dimethyltin(IV) complexes in solid state with Mes and Mops were characterized by means of elemental analyses and FTIR. The NMR (^1H, ^{13}C) spectra of the DMT–Mes complex exhibits the strongly distorted octahedron geometry around tin atom. Also, thermal analyses (TGA and DTA) were discussed. Thermodynamic parameters such as activation energy (E_a), pre-exponential factor (A), entropy of activation (ΔS^*) and free energy of activation (ΔG^*) have been calculated for each step, employing integral method Coats and Redfern. The reaction enthalpy (ΔH) is obtained from DTA data.

Keywords: Equilibrium studies; Dimethyltin(IV) complexes; Good's buffer; Mes; Mops; Effect of solvent and temperature; Thermodynamic parameters

1. Introduction

Organotin(IV) compounds are receiving increasing interest because of their biological and potential pharmaceutical applications as antitumour agents [1–8]. On the other hand, in recent years many organotin(IV) compounds have been tested for their in vitro activity against a large variety of tumor lines and have been found to be as effective or better than traditional heavy metal anticancer drugs, such as *cis*-platin [5,6]. In addition to the aforesaid applications organotin(IV) compounds are also of interest in view of the considerable structural diversity that they possess.

Good's buffers [9–11] are presently used routinely in biochemical and speciation studies under the assumption that they undergo little if any interaction with biologically (or environmentally) important metal ions. However, there has been an increase in reports on buffer interferences when most of Good's buffers were used in the presence of metal ions [12–18] many conflicting data and conclusions that were reported by investigators studying identical metal–cation protein systems (at the same pH in carefully executed experiments) might be due in part to the failure to include the presence of metal–buffer complexes [15]. These compounds (Good's buffers) contain hydroxyl, carboxylate or sulfydryl groups in addition to a primary nitrogen donor atom. Therefore, one might expect that metal complexes of these buffers would form in biochemical/environmental systems containing metal ions when these compounds are used to control the pH. On the other hand, it is known that 2-(*N*-morpholino)ethanesulfonic acid (Mes) and 3-(*N*-morpholino)-propanesulfonic acid (Mops) are important hydrogen ion buffers for biological media.

Investigation of the different complex species of the two biologically important compounds (dimethyltin(IV), M and zwitterionic buffers, L) are important. Therefore, a

* Corresponding author. Tel.: +20 927930654; fax: +20 927925393.
E-mail address: mmhm802004@yahoo.com (M.M.A. Mohamed).

0022-328X/$ - see front matter © 2007 Elsevier B.V. All rights reserved.
doi:10.1016/j.jorganchem.2006.12.035

systematic study for this complex system has been carried out. The effect of solvent and temperature on the complex formation equilibria were also investigated. This includes synthesis and characterization of the isolated solid complexes. Stoichiometry and stability of the various complex species in the complex system have been examined by pH-metric techniques. Also, experiments were carried out to deduce the decomposition pattern of DMT(IV)-Good's buffer under well controlled conditions by TGA, DrTGA and DTA techniques. Kinetic parameters for different decomposition stages are derived from the results and conclusions drawn from them are presented. The reaction enthalpy (ΔH) is obtained from DTA data.

2. Experimental

2.1. Materials and reagents

Dimethyltin(IV) dichloride was received from Aldrich Chemicals Co. The ligands (L) used were 2-(*N*-morpholino)ethanesulfonic acid (Mes) and 3-(*N*-morpholino)propanesulfonic acid (Mops). These materials were supplied from Fluka Chem. Co. Carbonate-free sodium hydroxide stock solutions were prepared by diluting the contents of BDH concentrated volumetric solution vials. These solutions were systematically checked by titration against potassium hydrogen phthalate. All solutions were prepared in deionized water.

3. Synthesis

Dimethyltin(IV) oxide (1 mmol) with (2-(*N*-morpholino)ethanesulfonate (Mes-Na salt) (2 mmol) or 3-(*N*-morpholino)propanesulfonate (Mops-Na salt) (2 mmol)) were prepared by dissolving Mes-Na or Mops-Na (2 mmol) in few drops of water and complete to 10 ml by adding absolute alcohol. The solution was added dropwise to 10 ml s of a stirred solution of dimethyltin(IV) oxide dissolved in absolute alcohol (1 mmol). The solution was stirred over night and the temperature adjusted to 40 °C in water bath. This mixture was slowly evaporates to obtain a volume of 10 ml. The mixture allowed to cool in refrigerator, a white precipitate formed. Then the precipitate was filtered off and washed sequentially with ethanol–water mixture and diethylether. Yield (70–80%) of white powder and recrystallized in ethanol. Anal. Calc. for $[(CH_3)_2Sn(Mes)OH]\cdot H_2O$ $(SnC_8H_{19}NO_5S]\cdot H_2O$; Decomp. point started at 100 °C; C, 25.4; H, 5.6; N, 3.7; S, 8.5. Found: C, 25.3; H, 5.4; N, 3.6; S, 8.4%. Anal. Calc. for $[(CH_3)_2Sn(Mops)OH]\cdot H_2O$ $(SnC_9H_{21}NO_5S]\cdot H_2O$; partial melt at 280 °C; C, 27.6; H, 5.9; N, 3.6; S, 8.2. Found: C, 27.4; H: 5.8; N; 3.5; S; 8.0%.

4. Apparatus

pH titrations were performed on a Metrohm 751 GPD titrino. The titroprocessor was calibrated with standard buffer solutions prepared according to NBS specification [19]. The titrations were carried out in a purified nitrogen atmosphere using a titration vessel described previously [20]. The temperature was maintained constant by a colora ultrathermostat. FTIR spectra were measured on an 80486-PC FTIR Shimadzu spectrophotometer using KBr pellets. NMR (^{1}H and ^{13}C) spectra were recorded on a VXR-300 Varian instrument operating at room temperature (respectively, at 300 MHz for ^{1}H and 75 MHz for^{13}C). Thermal analyses (TGA and DTA) were performed in nitrogen atmosphere with TGA-50 Shimadzu thermogravimetric analyzer and DTA-50 Shimadzu differential thermal analyzer. The operational characteristics are as follows:

- heating rate: 10 K min^{-1};
- sample size: 10–15 mg for TGA and 20 mg for DTA;
- atmosphere: nitrogen.
- temperature range: room temperature to 1200 °C.

5. Procedure and measuring techniques

The protonation constants of the ligands were determined by titrating 40 ml of ligand solution 2.5×10^{-3} M. The hydrolysis constants of dimethyltin(IV) were determined by titrating 40 ml of dimethyltin(IV) dichloride (2.5×10^{-3} M). The formation constant of organotin(IV) complexes were determined by titrating 40 ml of solution containing the ligand (2.5×10^{-3} M) and dimethyltin(IV) with concentrations 2.50×10^{-3} and 1.25×10^{-3} M. The titrations were performed in different temperatures and in dioxane–water solutions of different compositions. The ionic strength was adjusted to 0.1 M by $NaNO_3$. pK_w at different temperature and in dioxane–water solutions were determined as described previously [21]. For This purpose various amounts of standard NaOH solution were added to a solution containing 0.10 M $NaNO_3$. The [OH] was calculated from the amount of base added. The [H] was calculated from pH value. The product of [OH] and [H] was taken the mean values obtained in this way for the log concentration product are $\log K_w = -14.28$, -14.72, -15.13, -15.46, -15.70, -16.21 for 12.5%, 25.0%, 37.5%, 50.0%, 62.5%, 75.0% dioxane–water solutions and $\log K_w = -14.25$, -14.07, -13.89, -13.74 and 13.69 for 15, 20, 25, 30 and 35 °C, respectively.

The formed species in the studied systems were characterized by the general equilibrium processes (1), while the formation constants for these generalized species are given by Eq. (2).

$$pM + qL + rH \rightleftharpoons [M_pL_qH_r] \tag{1}$$

$$\beta_{pqr} = \frac{[M_pL_qH_r]}{[M]^p[L]^q[H]^r} \tag{2}$$

The calculations were performed using the computer program [22] MINIQUAD-75 loaded on Pentium II-233 computer. The stoichiometries and stability constants of the complexes formed were determined by trying various possible composition models for the system studied.

The model selected gave the best statistical fit and was chemically consistent with the titration data without giving any systematic drifts in the magnitudes of various residuals, as described elsewhere [22]. The concentration distribution diagrams were obtained using the program SPECIES [23].

6. Results and discussion

6.1. Solution-phase investigations

Dimethyltin(IV) cation is known [21,24–28] to form stable and water soluble mono- and polynuclear hydroxo species (see Table 1) in the whole pH-range studied. Since the hydroxide ion and the studied ligands are in stronge competition for the metal ion, these species were always taken into consideration in the equilibrium systems.

The acid dissociation constants of Mes and Mops were determined under the same experimental conditions of ionic strength and temperature (See Table 1). These constants should be taken into consideration during the evaluation of the pH-metric data. It is found that $\log \beta_{011} = 6.06$ and 7.12 for Mes and Mops, respectively, [29]. The protonation constant for the zwitterionic buffers (Good's buffer) clearly indicate the formation of different basicity of tertiary amine. This due to the substitution of increasingly larger alkyl chains between the tertiary amine group and the sulfonic group, the addition of hydroxyl groups on the molecule, or other modifications to the backbone N-substituted structure.

The displayed titration curves for the complex solutions with (1:1 and 2:1) ligand to metal ratio clearly indicate the formation of different kinds of complexes (c.f. Fig. 1). The best fit of the titration curves were obtained when complexes ML, MLH_{-1}, MLH_{-2} and MLH_{-3} were expected beside the hydrolysis products of the dimethyltin(IV) cation, Table 1.

The potentiometric titration curves of dimethyltin(IV) complexes against both of Mes and Mops with different stiochiometric species (1:1 and 1:2, metal: ligand) of these systems started at pH ~3.0. At this pH the sulphonic group was already deprotonated and do not play a role in mode of coordination with DMT(IV) anion. By increasing pH the Mes and Mops react with DMT(IV) as a monodentate ligand forming a deprotonated complex ML. ML is competed with hydroxo complex at lower pH ~ 3.0 (Fig. 2). At higher pH's further deprotonation was observed leading to form mixed-hydroxo complex species MLH_{-1}, MLH_{-2} and MLH_{-3}.

7. Effect of temperature

The thermodynamic parameters $\Delta H°$, $\Delta S°$ and $\Delta G°$ were obtained by linear least square fit of $\ln K^T$ versus $1/T$ leading to an intercept $\Delta S°/R$ and a slope $-\Delta H°/R$. The results obtained are summarized in Table 2 and explained as follows:

Table 1
Formation constants of dimethyltin(IV) (DMT) complexes in water at different temperature

System[a]	Temperature (°C)	p	q	r[b]	Log β[c]	S[d]
DMT	15	1	0	−1	−3.56(0.01)	5.4E−8
		1	0	−2	−9.05(0.01)	
		1	0	−3	−19.79(0.04)	
		1	0	−4	−30.41(0.04)	
		2	0	−2	−4.23(0.01)	
		2	0	−3	−9.52(0.01)	
		2	0	−4	−15.23(0.01)	
Mes		0	1	1	6.22(0.01)	1.8E−8
		1	1	0	6.18(0.01)	1.4E−8
		1	1	−1	2.47(0.01)	
		1	1	−2	−3.41(0.01)	
		1	1	−3	−11.74(0.05)	
DMT	20	1	0	−1	−3.31(0.01)	6.1E−8
		1	0	−2	−8.64(0.01)	
		1	0	−3	−19.27(0.05)	
		1	0	−4	−39.71(0.02)	
		2	0	−2	−3.77(0.01)	
		2	0	−3	−8.91(0.02)	
		2	0	−4	−14.44(0.01)	
Mes		0	1	1	6.16(0.01)	2.4E−8
		1	1	0	6.07(0.01)	1.9E−9
		1	1	−1	2.62(0.01)	
		1	1	−2	−3.19(0.01)	
		1	1	−3	−11.61(0.02)	
DMT	25	1	0	−1	−3.03(0.01)	4.3E−8
		1	0	−2	−8.21(0.01)	
		1	0	−3	−18.73(0.03)	
		1	0	−4	−29.54(0.02)	
		2	0	−2	−3.12(0.01)	
		2	0	−3	−8.13(0.02)	
		2	0	−4	−13.59(0.02)	
Mes		0	1	1	6.06(0.01)	6.7E−9
		1	1	0	5.91(0.01)	2.9E−8
		1	1	−1	2.73(0.01)	
		1	1	−2	−3.01(0.02)	
		1	1	−3	−11.56(0.04)	
Mops		0	1	1	7.12(0.01)	3.6E−7
		1	1	0	7.29(0.06)	3.2E−7
		1	1	−1	2.71(0.04)	
		1	1	−2	−3.81(0.04)	
		1	1	−3	−11.86(0.08)	
DMT	30	1	0	−1	−2.81(0.01)	6.6E−8
		1	0	−2	−7.91(0.02)	
		1	0	−3	−18.38(0.05)	
		1	0	−4	−28.71(0.02)	
		2	0	−2	−2.87(0.02)	
		2	0	−3	−7.84(0.04)	
		2	0	−4	−13.06(0.04)	
Mes		0	1	1	5.96(0.01)	1.9E−8
		1	1	0	5.83(0.04)	2.0E−8
		1	1	−1	2.79(0.01)	
		1	1	−2	−2.89(0.01)	
		1	1	−3	−11.59(0.07)	
DMT	35	1	0	−1	−2.49(0.02)	6.9E−8
		1	0	−2	−7.54(0.02)	
		1	0	−3	−17.95(0.06)	
		1	0	−4	−28.20(0.03)	
		2	0	−4	−2.27(0.03)	

(continued on next page)

Table 1 (*continued*)

System[a]	Temperature (°C)	*p*	*q*	*r*[b]	Log *β*[c]	*S*[d]
		2	0	−3	−7.11(0.04)	
		2	0	−4	−12.34(0.04)	
Mes		0	1	1	5.88(0.01)	1.9E−8
		1	1	0	5.69(0.08)	6.3E−8
		1	1	−1	2.79(0.01)	
		1	1	−2	−2.82(0.01)	
		1	1	−3	−11.59(0.03)	

[a] Mes denote 2-(*N*-morpholino)ethanesulfonic acid, Mops denote 3-(*N*-morpholino)-propanesulfonic acid.

[b] *p*, *q* and *r* are the stoichiometric coefficient corresponding to dimethyltin(IV), Good's buffers and H^+, respectively.

[c] Standard deviations are given in parentheses.

[d] Sum of square of residuals.

(a) The formation constants for the hydrolyzed species of dimethyltin(IV) discussed in the previous work [21].
(b) The protonation reactions of tertiary amine site of Mes is exothermic and the entropy is positive. This means that the protonation constant of Mes is ordered and favoured with increasing temperature (Fig. 3).
(c) The complex-formation of Mes with DMT is exothermic for ML, MLH_{-1} and MLH_{-2} species and endothermic for MLH_{-3} species. This may be explained statistically based on the presumption that more coordination sites are available for binding ML, MLH_{-1} and MLH_{-2} species (Fig. 4). The formation of the MLH_{-1} species is more exothermic than ML species. This means than the hydroxo complex is more favoured than the deprotonated complex species, due to the high affinity of dimethyltin(IV) to form hydroxo complex.

8. Effect of solvent

Traditionally, water has been considered as the solvent which best represents the biological conditions. Although this is a general assumption, a lower polarity has been detected in some biochemical micro-environments, such as active sites of enzymes and side chains in proteins, sometimes hidden in lower dielectric cavities [30–34]. In these cases, the selection of other solvents seems more recommendable in order to emulate property the medium's real features. Careful examination of the medium effect on the equilibrium constants. Table 3 is summarized in the following:

(a) Log *β* 011 of Mes (tertiary amine), as well as the hydrolysis constants of dimethyltin(IV) decrease linearly with increase of dioxane proportion in the medium, Fig. 5. This may be correlated with the ability of

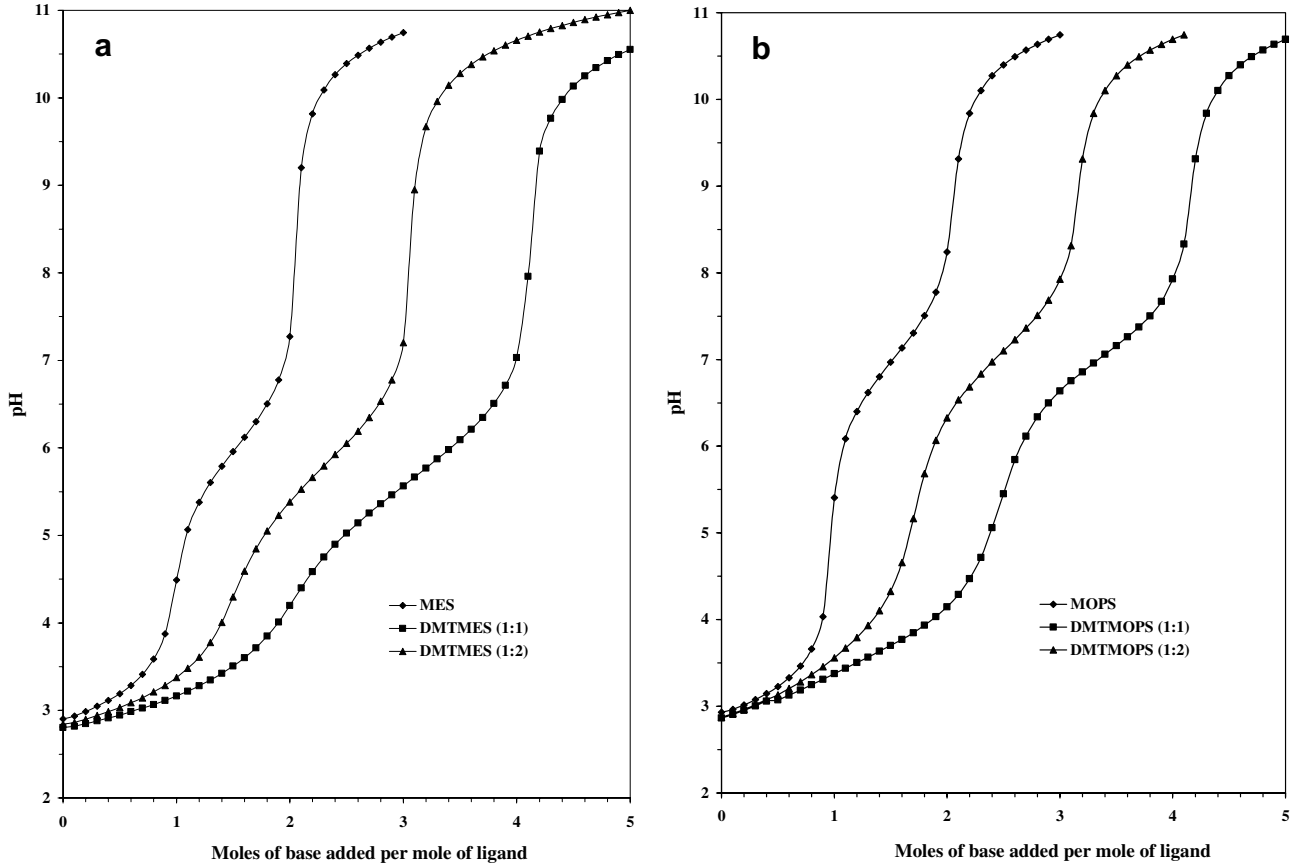

Fig. 1. Potentiometric titration curves of the DMT–Mes (a) and DMT–Mops systems (b).

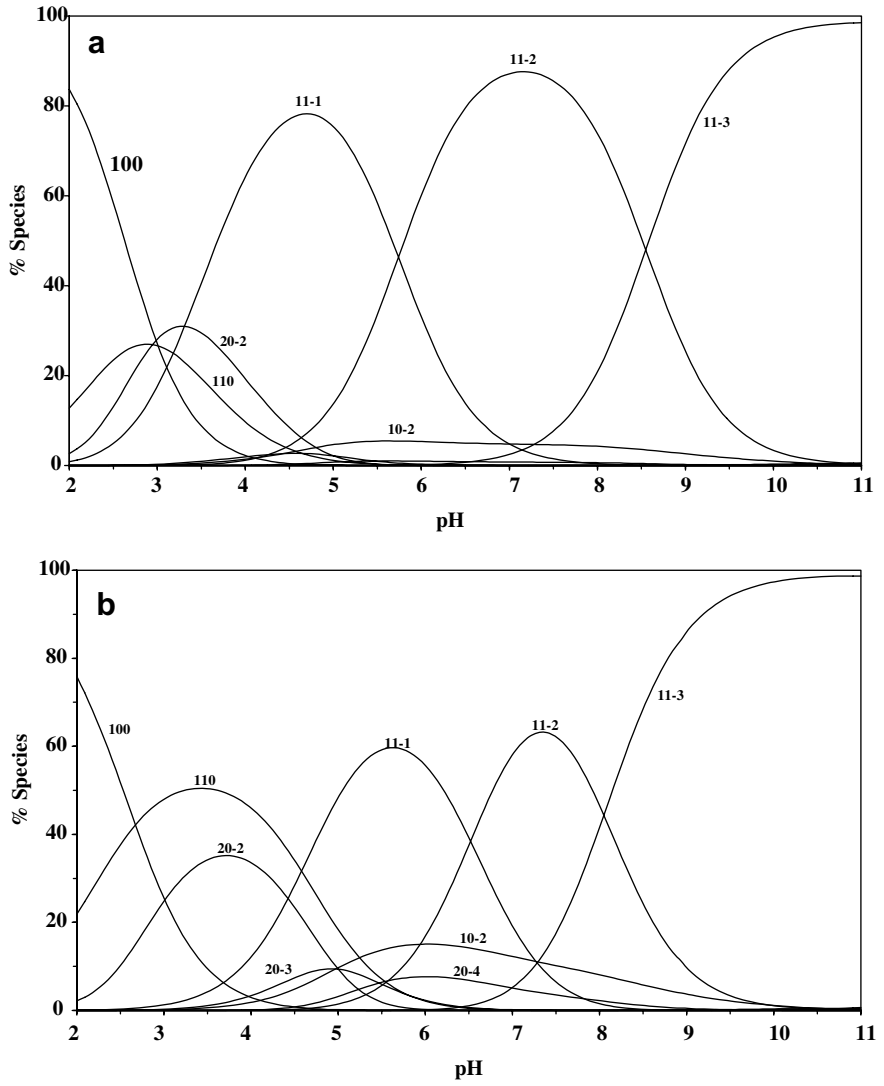

Fig. 2. Species distribution curves in the dimethyltin(IV)–Mes (a), and Mops (b) systems. [M] = 2.50 mmol, [L] = 2.50 mmol. The notation of the different species corresponds to the *pqr* values of the corresponding complex $M_pL_qH_r$.

Table 2
Thermodynamic parameters for the equilibria of dimethyltin(IV) complexes[a]

Equilibrium[b]	$\Delta H°$ (kJ Mol^{-1})	$\Delta S°$ (J K^{-1} Mol^{-1})	$\Delta G°$ (kJ Mol^{-1})
Mes			
(1) $L^- + H^+ \leftrightharpoons LH$	−39.80(0.5)	9(1)	−42.50(0.7)
DMT–Mes			
(2) $M^{2+} + L^- \leftrightharpoons ML^+$	−41.47(0.4)	−26(1)	−33.85(0.9)
(3) $ML^+ + OH^- \leftrightharpoons MLH_{-1}$	−69.19(0.01)	−170(1)	−18.54(1.2)
(4) $MLH_{-1} + OH^- \leftrightharpoons MLH_{-2}$	−22.77(0.03)	34(1)	−32.76(0.8)
(5) $MLH_{-2} + OH^- \leftrightharpoons MLH_{-3}$	38.39(0.07)	292(2)	−48.80(1.1)

[a] DMT or M denote Dimethyltin(IV), Mes denote 2-(*N*-morpholino)ethanesulfonic acid, Mops denote 3-(*N*-morpholino)propanesulfonic acid; standard deviations are given in parentheses.
[b] Stepwise formation constants.

a solvent of relatively low dielectric constant to decrease the electrostatic forces between the proton and ligand anions in case of ligand dissociation and that between the proton and hydrolysed form of organotin(IV).

(b) The variation of the stability constants of the DMT complexes with Mes as a function of solvent composition is exhibited in Fig. 6. The stability constants of the MLH_{-1} species with Mes increase with increasing dioxane proportion. On the other hand, ML,

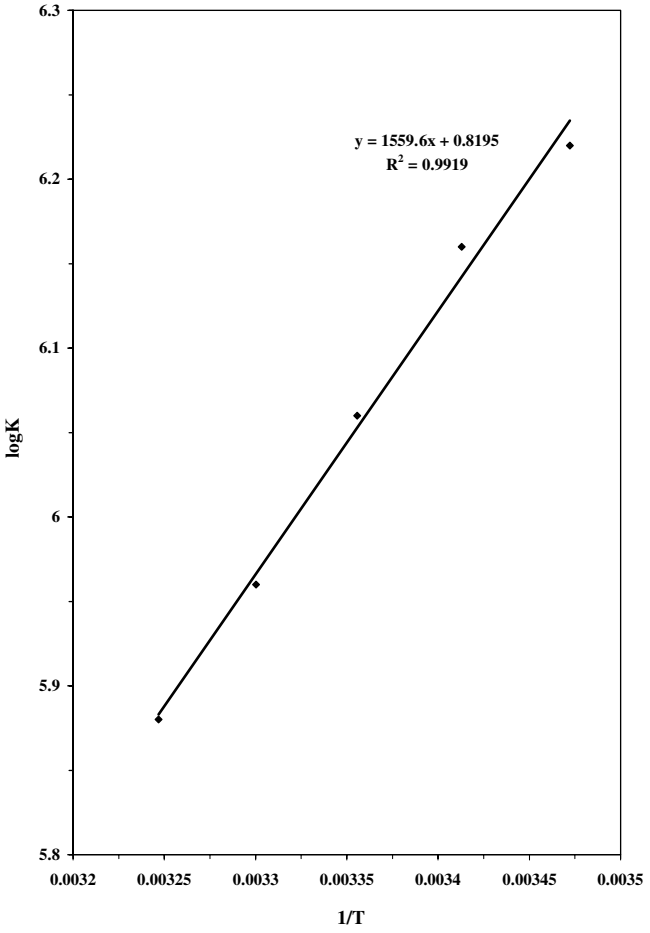

Fig. 3. Plot of log K vs. $1/T$ of the Good's buffer (Mes) system.

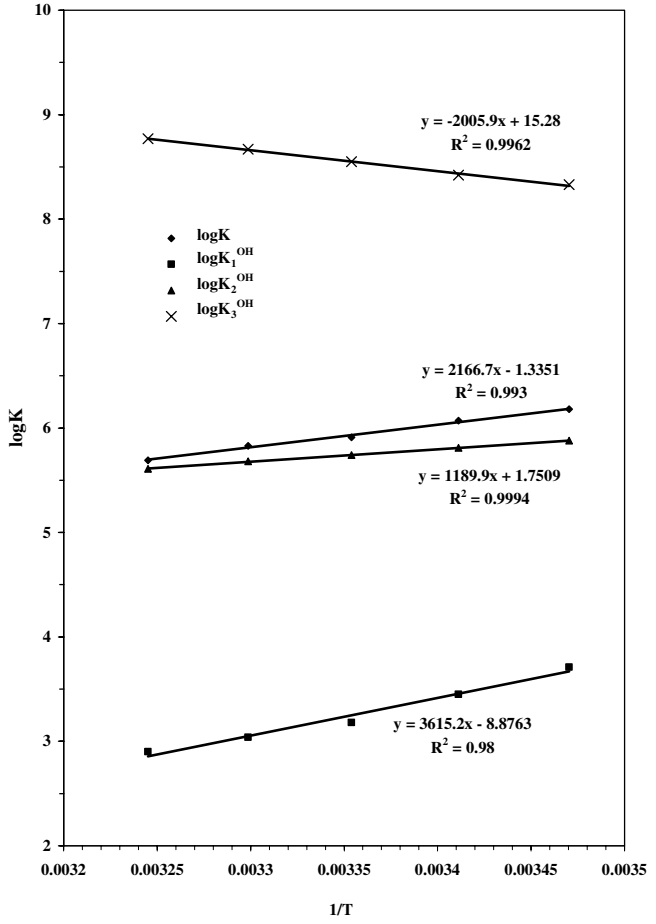

Fig. 4. Plot of log K vs. $1/T$ of the DMT–Good's buffer (Mes) systems.

MLH_{-2}, MLH_{-3} species decreases with increasing dioxane proportion. This may be explained on the premise that the MLH_{-1} species involve neutralization charges.

9. Solid-phase investigations

The characteristic IR absorption bands of the complexes and the corresponding free ligands (Mes and Mops) in the region 4000–400 cm^{-1} are given in Table 4. The ν(OH) of the free ligands appears at frequencies (3387 and 3359 cm^{-1} for Mes and 3447 cm^{-1} for Mops), indicating the presence of these OH groups in stronger H-bonding [18,35]. The stretching vibrations of the SO_4^- groups at (multiple peaks from 2740 to 2500 cm^{-1}) and (multiple peaks from 2722 to 2523 cm^{-1}) for Mes and Mops, respectively, indicating that all of the ligands studied here have a zwitterion structure.

New very broad band at 3450 and 3416 cm^{-1} appearing for the synthesized complexes may be due to (H_2O and/or hydroxo complex) as discussed in the thermal analyses part. The characteristic bands of OH stretching vibrations did not appear in the IR spectra of the complexes which may be due to participation as coordination site. The multiple bands of SO_3^- groups suffer a lower shift to one frequency at 2470 and 2693 cm^{-1} for Mes and Mops, respectively. This behaviour indicates that the ligands (Mes or Mops) are coordinated to the dimethyltin(IV) moiety through the SO_3^- and tertiary amine groups of the ligand.

The assignment of ν(Sn–C), ν(Sn–O) and ν(Sn–N) are consistent with values reported in the literature [36]. However, observation of both ν_{as}(Sn–C), ν_s(Sn–C) bands in the infrared spectra of all compounds studied rules out the planar arrangement for the Sn–C skeleton.

^{1}H NMR and ^{13}C NMR spectral data of DMT–Mes complex has been recorded in Table 5. The proton of –OH group of the Mes gives signal at δ (13.44 ppm) and which is absent in the DMT complex indicating the coordination of tin with the oxygen atom. The protons of the carbon atoms around the nitrogen atom in the morpholine ring and ethanesulfonate show marked shifting due to the coordination of imino group with tin atom. The large change in ^{13}C chemical shifts in the spectra of the complex was compared to the Mes ligand clearly shows the coordination of the (imino and hydroxyl groups) to the tin atom. The identification of dimethyltin(IV) in the complex confirms the complexation.

Table 3
Formation constants of dimethyltin(IV) complexes in dioxane–water solutions of different compositions

System[a]	Dioxane (%)	*l*	*p*	*q*[b]	Log *β*[c]	*S*[d]
DMT	12.5	1	0	−1	−3.27(0.01)	1.3E−7
		1	0	−2	−8.70(0.02)	
		1	0	−3	−19.53(0.06)	
		1	0	−4	−30.09(0.03)	
		2	0	−2	−3.68(0.02)	
		2	0	−3	−8.94(0.05)	
		2	0	−4	−14.52(0.04)	
Mes		0	1	1	6.13(0.01)	2.2E−8
		1	1	0	5.94(0.01)	2.9E−9
		1	1	−1	2.61(0.01)	
		1	1	−2	−3.53(0.01)	
		1	1	−3	−11.58(0.04)	
DMT	25.0	1	0	−1	−3.39(0.00)	1.0E−8
		1	0	−2	−8.99(0.01)	
		1	0	−3	−19.83(0.01)	
		1	0	−4	−31.30(0.01)	
		2	0	−2	−3.92(0.01)	
		2	0	−3	−9.27(0.04)	
		2	0	−4	−15.11(0.03)	
Mes		0	1	1	6.04(0.01)	1.6E−8
		1	1	0	5.85(0.02)	4.6E−9
		1	1	−1	2.34(0.01)	
		1	1	−2	−3.57(0.01)	
		1	1	−3	−11.81(0.04)	
DMT	37.5	1	0	−1	−3.53(0.01)	1.4E−8
		1	0	−2	−9.23(0.01)	
		1	0	−3	−20.18(0.02)	
		1	0	−4	−31.83(0.01)	
		2	0	−2	−4.17(0.01)	
		2	0	−3	−9.61(0.03)	
		2	0	−4	−15.59(0.03)	
Mes		0	1	1	5.93(0.01)	2.4E−8
		1	1	0	5.77(0.06)	1.0E−7
		1	1	−1	2.68(0.01)	
		1	1	−2	−2.85(0.01)	
		1	1	−3	−10.59(0.03)	
DMT	50.0	1	0	−1	−3.60(0.01)	2.8E−8
		1	0	−2	−9.43(0.01)	
		1	0	−3	−20.58(0.02)	
		1	0	−4	−32.52(0.02)	
		2	0	−2	−4.30(0.01)	
		2	0	−3	−9.78(0.04)	
		2	0	−4	−16.03(0.04)	
Mes		0	1	1	5.82(0.01)	5.1E−8
		1	1	0	5.61(0.01)	2.7E−9
		1	1	−1	2.04(0.01)	
		1	1	−2	−4.29(0.01)	
		1	1	−3	−12.24(0.02)	
DMT	62.5	1	0	−1	−3.68(0.01)	8.7E−8
		1	0	−2	−9.62(0.02)	
		1	0	−3	−20.89(0.04)	
		1	0	−4	−33.26(0.05)	
		2	0	−2	−4.47(0.01)	
		2	0	−3	−9.90(0.03)	
		2	0	−4	−16.51(0.04)	
Mes		0	1	1	5.71(0.01)	1.0E−7
		1	1	0	5.44(0.04)	2.0E−8
		1	1	−1	1.61(0.02)	
		1	1	−2	−5.20(0.02)	
		1	1	−3	−13.18(0.04)	
DMT	75.0	1	0	−1	−3.98(0.02)	1.4E−7
		1	0	−2	−9.93(0.05)	
		1	0	−3	−21.35(0.09)	
		1	0	−4	−33.74(0.08)	
		2	0	−2	−4.90(0.01)	
		2	0	−3	−10.10(0.01)	
		2	0	−4	−16.96(0.02)	
Mes		0	1	1	5.62(0.01)	1.5E−7
		1	1	0	5.22(0.07)	1.1E−7
		1	1	−1	2.08(0.01)	
		1	1	−2	−4.03(0.02)	
		1	1	−3	−11.82(0.03)	

[a] Mes denote 2-(*N*-morpholino)ethanesulfonic acid, Mops denote 3-(*N*-morpholino)-propanesulfonic acid.
[b] *p*, *q* and *r* are the stoichiometric coefficient corresponding to dimethyltin(IV), Good's buffers and H^+, respectively.
[c] Standard deviations are given in parentheses.
[d] Sum of square of residuals.

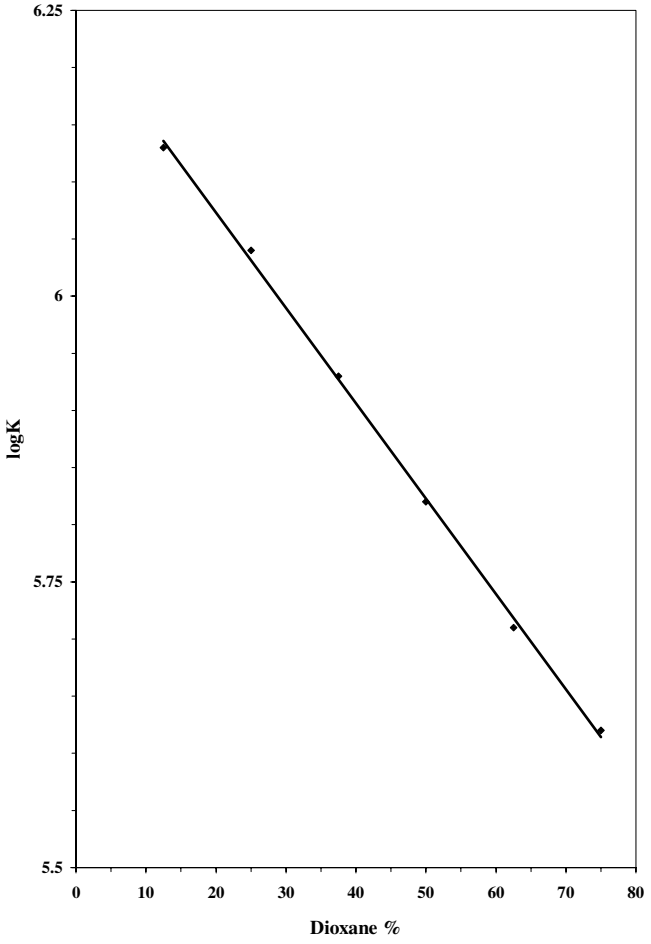

Fig. 5. Effect of dioxane on the log K of Good's buffer (Mes).

The ^{13}C NMR spectrum to complex DMT–Mes showed a $^1J(^{119}Sn–^{13}CH_3)$ coupling constant of 607.11 Hz and the ^1H NMR spectrum showed at δ 0.64 corresponding to

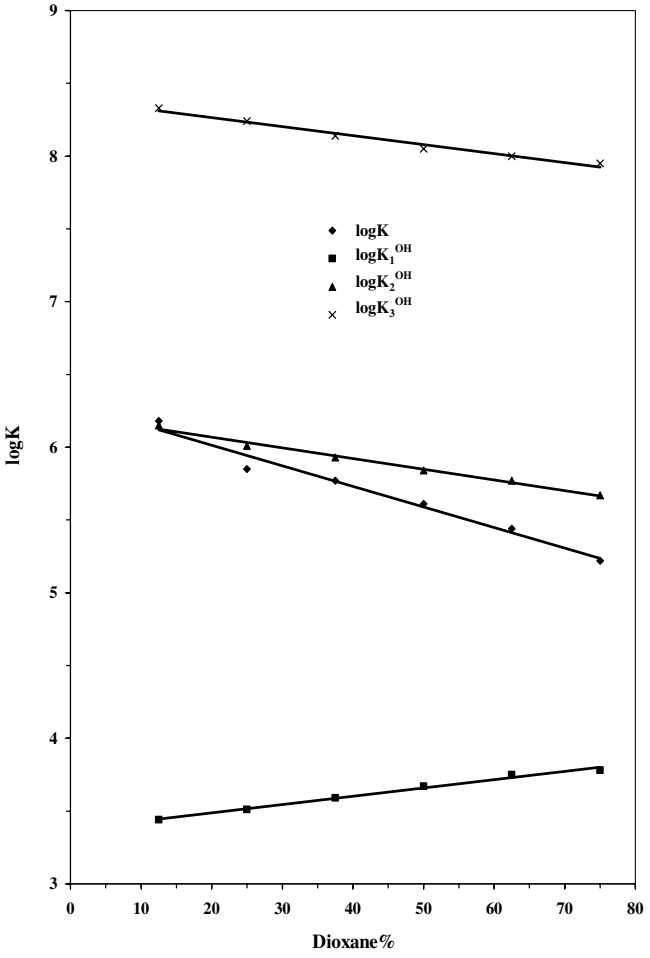

Fig. 6. Effect of dioxane on the logK of DMT–Mes complex.

the protons of methyl groups attached to the tin atom. ^{119}Sn and ^{117}Sn satellites due to coupling ^{119}Sn–^{1}H and ^{117}Sn–^{1}H were also observed. It is well known that the magnitude of $^{2}J(^{119}\text{Sn}–^{1}\text{H})$ spin-spin coupling constant is function of the coordination number in dimethyltin(IV) compounds. These (^{2}J) coupling constants data can be used to estimate the CH_3-Sn–CH_3 angle in complex DMT–Mes, and according to the literature [37,38], two empirical equations can be set up for this estimate:

$$^{1}J(^{119}\text{Sn}—^{13}\text{CH}_3) = 11.4\theta - 875 \quad (3)$$

$$\theta = 0.0161\{^{2}J(^{119}\text{Sn}—\text{CH}_3)\}^2 - 1.32\{^{2}J(^{119}\text{Sn}—\text{CH}_3)\} + 133.4 \quad (4)$$

Using ^{1}J into Eq. (3) and ^{2}J into Eq. (4), one finds values of θ of 130 and (132.18 and 132.82 for ^{117}Sn–^{1}H/^{119}Sn–^{1}H), respectively. These angles values might suggests that in solution the dimethyltin derivative was a distorted trans octahedral complex and the basic structural features of the solid-state phase remain in D_2O solution.

Similar results were reported for octahedral complexes with analogous trans arrangement, namely $[Me_2Sn(dtc)_2]$ [39] [$^{2}J(^{119}$Sn–$CH_3)$ 84 Hz and $^{1}J(^{119}$Sn–$^{13}CH_3)$ 670 Hz], $[Me_2SnCl_2(DMSO)_2]$ [37] [$^{2}J(^{119}$Sn–$CH_3)$ 86 Hz], $[Me_2Sn(CH_3COO)_2]$ [40] [$^{2}J(^{119}$Sn–$CH_3)$ 82 Hz] and [$^{2}J(^{119}$Sn–$CH_3)$ 83 Hz] [41] Me_2Sn(Me2-Pymt)$_2$, where Hdtc = ditiocabamic acid, DMSO = dimethyl-sulfoxide and Me2PymtH = 4,6-dimethyl-pyrimidine-2-thione.

10. TGA, DrTG and DTA analyses

10.1. Thermogravimetric studies (TGA)

The TGA for the complexes was carried out within a temperature ranged from room temperature up to 1200 °C. The determined temperature ranges, percent losses in mass and thermal effects accompanying the

Table 4
IR absorption bands of the free ligands and the DMT complexes in KBr (cm^{-1})

Complexes	ν_{H_2O}, ν_{OH}	ν_{NH^+}	ν_{SO_3}	$\nu_{S=O}$	$\nu_{C–N}$	$\nu_{C–S}$	$\nu_{Sn–N}$	$\nu_{Sn–O}$	$\nu_{as(Sn–C)}$	$\nu_{s(Sn–C)}$
Mes · H_2O $[C_6H_{13}NO_4S]$ · H_2O	3387	3359	2740, 2654, 2614, 2500	1226, 1185, 1123, 1083, 1037	909, 872	635	–	–	–	–
[DMT–Mes(OH)] · H_2O $[SnC_8H_{18}NO_4SOH]$ · H_2O	3450	–	2470	1189, 1062	904, 865	640	429	574	552	519
Mops $C_7H_{15}NO_4S$	3447	3447	2722, 2709, 2647, 2523	1216, 1165, 1118, 1079, 1036	910, 881	614	–	–	–	–
[DMT–Mops(OH)] · H_2O $[SnC_9H_{20}NO_4SOH]$ · H_2O	3416, 3310	–	2730, 2693	1192, 1139, 1113, 1046	917, 860	680	432	580	550	520

Table 5
^{1}H NMR and ^{13}C NMR data (δ ppm) of Mes and dimethyltin(IV) complex

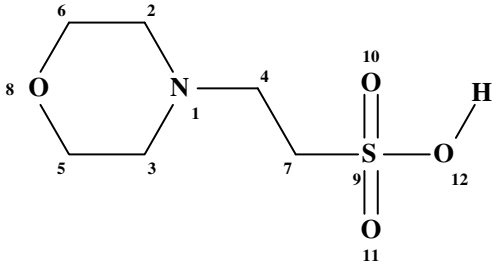

System						
^{1}H NMR data	2,3	4	5,6	7	12	C–Sn–C
$C_6H_{13}NO_4S$	2.25	3.13	3.01	2.86	13.44	
$[SnC_8H_{18}NO_4SOH]\cdot H_2O$	2.87	3.80	3.18	2.64		$0.64\,^{2}J(^{117}Sn–^{1}H)/^{2}J(^{119}Sn–^{1}H) = 81.06/81.54$
^{13}C NMR data						
$C_6H_{13}NO_4S$	54.52	51.85	65.62	46.85	–	
$[SnC_8H_{18}NO_4SOH]\cdot H_2O$	49.67	44.76	63.45	35.11	–	$-0.36\,^{1}J(^{119}Sn–^{13}CH_3) = 607.32$

changes in the solid complexes on heating are given in Table 6, which revealed the following findings. The dimethyltin(IV) complex of Mes gives four stages of decomposition pattern. The first stage, within the temperature range of 89–112 °C, represents the loss of water molecules of hydration and CH_2O, due to the decomposition point of the DMT–Mes complex starts to decompose ≈100 °C (estimated mass loss 13.15%, theoretical 12.71%), Fig. 7. The activation energy of this dehydration step is 155.1 kJ/mol (Table 7). The second stage (319–357 °C) represents the loss of C_3H_6 molecule with an estimated mass loss of 11.17% (theoretical 11.13%). The third decomposition stage, which begins at 595 up to 610°C and reasonably accounted to the loss of CH_3 molecule (estimated mass loss 3.95%, theoretical 3.98%). The last stage of decomposition within the temperature range 1046–1152°C with an estimated mass loss 15.10% (theoretical 15.34%) is accounted to the loss of C_3H_8N molecule leaving $1/2Sn(SO_4)_2\cdot SnO_2$ residue (estimated remaining mass 56.71%, theoretical 56.81%).

The thermogram of dimethyltin(IV)–Mops complex shows that at a temperature of 26–72 °C, only the one water molecule of hydration are lost with an estimated mass loss of 4.49% (theoretical 4.60%), Fig. 8. The activation energy of the thermal dehydration of this complex is 155.2 kJ/mol. The second (278–296 °C) and third (312–319 °C) steps involve the loss of C_4H_8O and C_3H_6N molecules, respectively. The last step (385–513 °C) is attributed to the loss of C_2H_6 molecule (estimated mass loss 7.65%, theoretical 7.93%) leaving basic metal sulphate residue ($1/2Sn(SO_4)_2\cdot SnO_2$) as the product of decomposition. The estimated mass losses corresponding to all temperature ranges are 45.01% (theoretical 45.23%) and 51.65% (theoretical 51.50%), respectively.

Comparison of the estimated mass losses of DMT–Mes complex with those of DMT–Mops, the thermogram indicate that DMT–Mes complex (temperature range for all steps from 89 up to 1152 °C) is thermally stable than those of DMT–Mops complex (temperature range for all steps from 26 up to 513 °C). The DMT–Mes form six membered

Table 6
Percentage mass loss of dimethyltin(IV) complexes with Mes and Mops

Temperature range	Step	Temperature range	T_i K	% Mass loss found (Calc.)	Estimated
DMT–Mes					
$[SnC_8H_{18}NO_4SOH]\cdot H_2O$	I	89–112	375.05	12.71(13.15)	$-H_2O$ $-CH_2O$
	II	319–357	614.55	11.13(11.17)	$-C_3H_6$
	III	595–610	853.55	3.98(3.95)	$-CH_3$
	IV	1046–1152	1379.85	15.34(15.10)	$-C_3H_8N$
% Metal residual				56.81(56.71)	$1/2(Sn(SO_4)_2\ SnO_2)$
DMT–Mops					
$[SnC_9H_{20}NO_4SOH]\cdot H_2O$	I	26–72	332.45	4.60(4.49)	$-H_2O$
	II	278–296	562.75	18.39(18.49)	$-C_4H_8O$
	III	312–319	592.65	14.31(14.38)	$-C_3H_6N$
	IV	385–513	727.05	7.93(7.65)	$-C_2H_6$
% Metal residual				54.77(54.99)	$1/2(Sn(SO_4)_2\ SnO_2)$

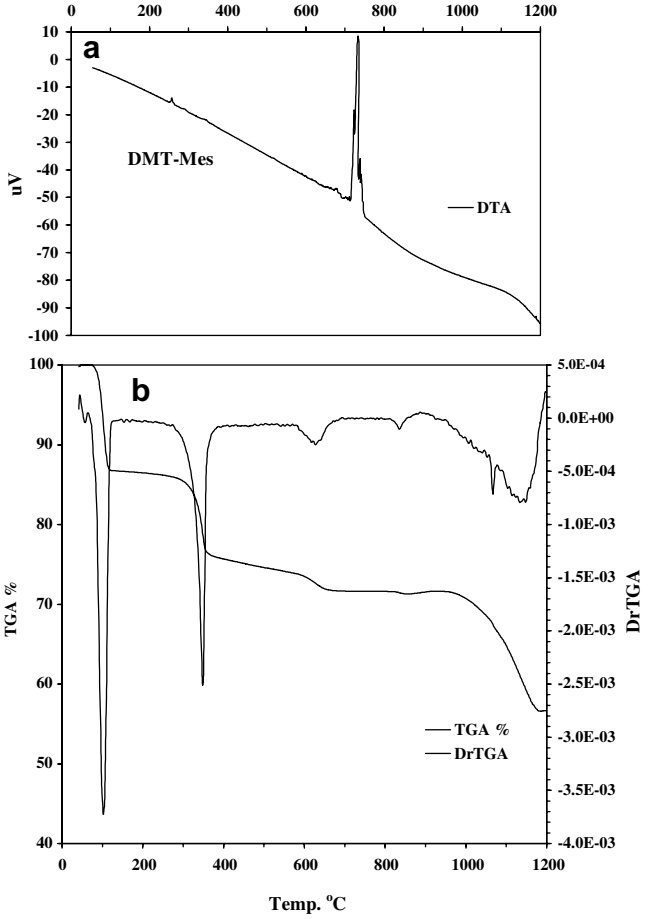

Fig. 7. TGA, DrTGA and DTA curves of the DMT–Mes complex.

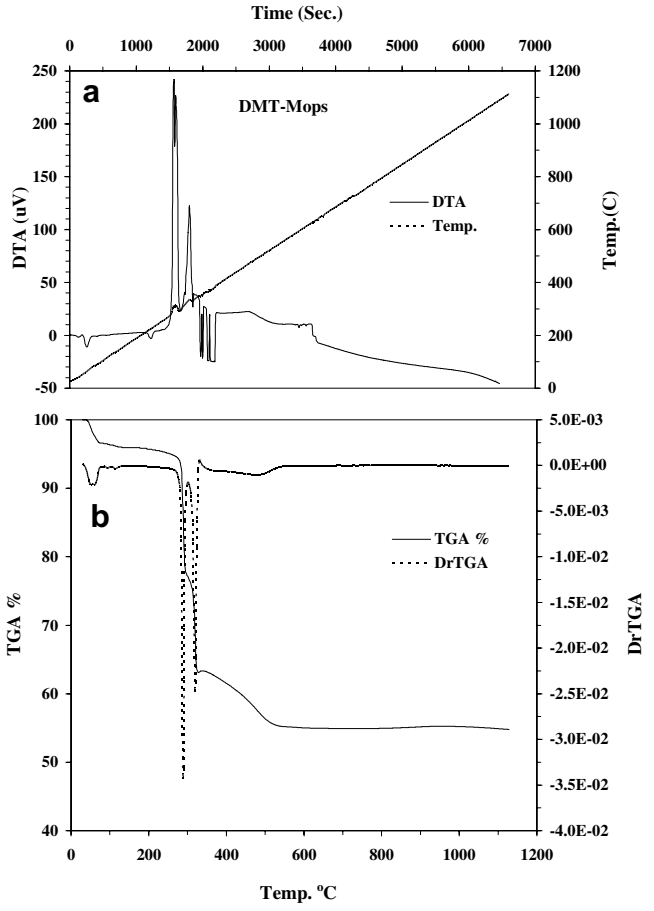

Fig. 8. TGA, DrTGA and DTA curves of the DMT–Mops complex.

Table 7
Calculation of the heat of reaction (ΔH) from DTA technique

Temperature range	Step	Peak temperature	$-\Delta H$ (J)	$-\Delta H$ (kJ/mol)
DMT-Mes				
704–740	I	733.7	−5.13	−96.98
DMT-Mops				
50–75	I	63	0.71	14.00
208–238	II	223.2	0.43	8.45
260–313	III	312.4	−16.39	−321.20
313–335	IV	335.0	−5.65	−110.68
344–392	V	380.0	6.12	119.90
650–658	VI	649.4	3.19	62.50
707–726	VII	700.7	−1.89	−37.05

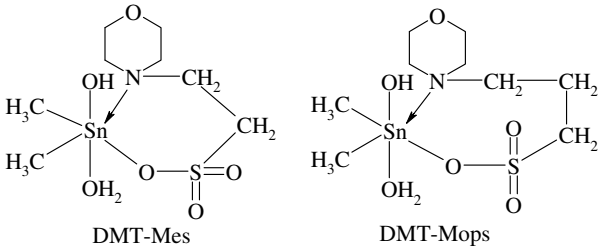

Scheme 1. Structural formulae of dimethyltin(IV)-Good's buffer.

chelate ring is higher than those involving seven membered, as in DMT–Mops. This may be explained on the premise that the six-membered ring is more favoured energetically than the seven-membered rings. On the basis of the above observations, the following structures may be proposed for the above studied complexes (Scheme 1).

10.2. Differential thermal analysis

The peak area in DTA depends upon the mass of sample (m) used. The heat of reaction or enthalpy change (ΔH) concerned, plus additional factors like sample geometry and thermal conductivity [42]. The latter two factors give rise to an empirical constant (K) such that:

$$\text{Peak area}(A) = \pm K \cdot \Delta H \cdot m$$

We shall use the positive sign for endothermic reactions, in which $\Delta H > 0$, and the negative sign for exothermic reactions in which $\Delta H < 0$. Calculation the heat of reaction or enthalpy change (ΔH) by using TG-Analysis program (copyright (1991–1994) by Shimadzu Crop, Table 7).

Endotherm in DTA of DMT–Mes complex shows degrading curve displayed a change from 25 up to 704 °C, Fig. 7a. These step followed a strong exothermic process observed in the DTA curve from 704 to 740 °C

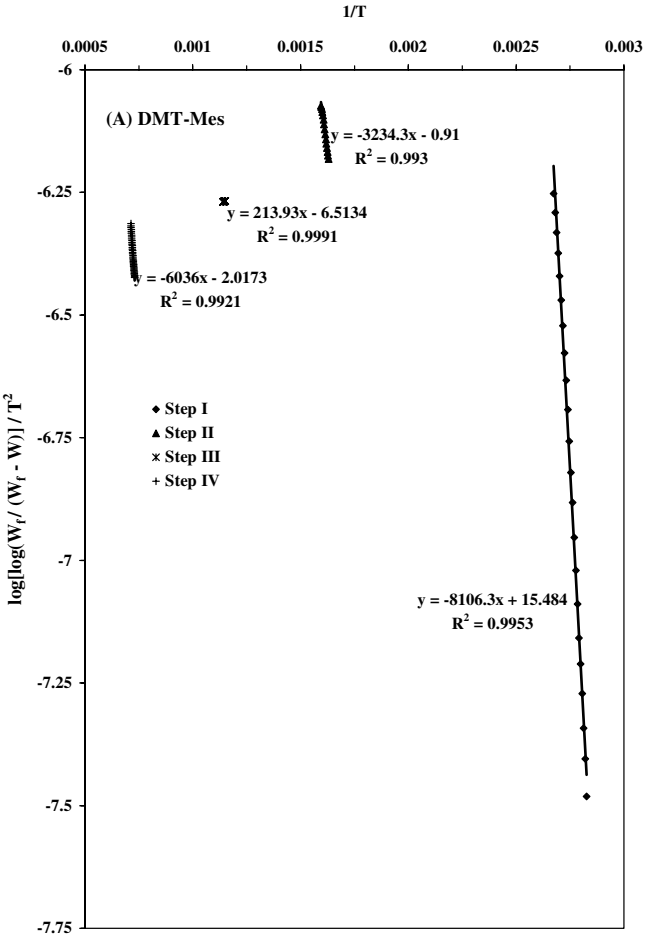

Fig. 9. Plot $\log[\log(W_f)/(W_f - W)/T^2]$ vs. $1/T$ of the DMT–Mes complex.

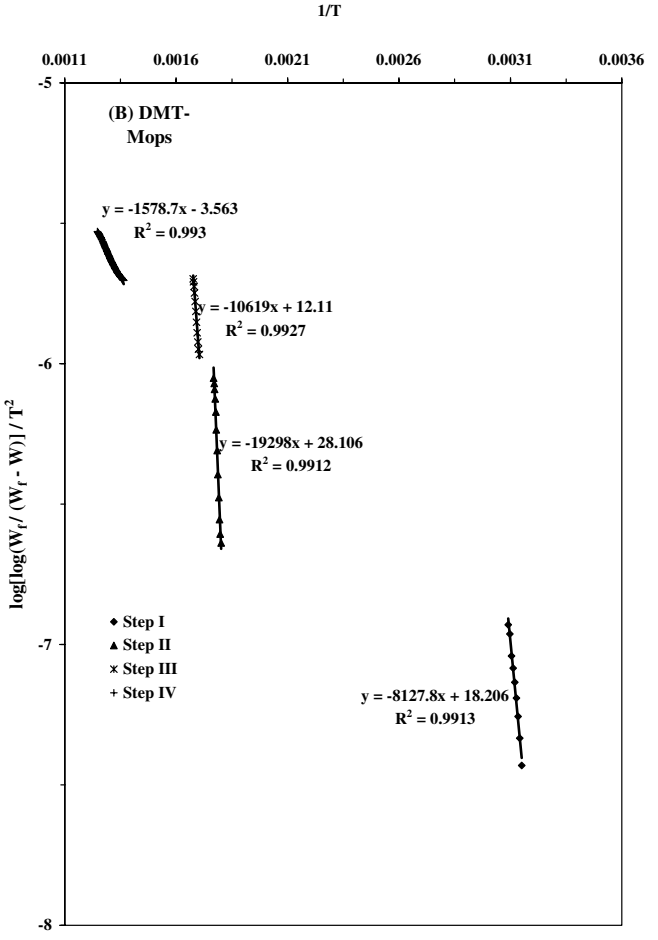

Fig. 10. Plot $\log[\log(W_f)/(W_f - W)/T^2]$ vs. $1/T$ of the DMT–Mops complex.

but there is no change in DrTGA indicating that there is some phase changes or changes in crystallinity of the species. This might also be due to the transition [43] of the anhydrous compound from the amorphous state to crystalline state along with some partial decomposition of the complex Figs. 9 and 10.

The DTA of complex DMT–Mops is shown in Fig. 8a. The transitions observed in the DTA curve correspond to the transitions observed in the TGA curve. Three exothermic and four endothermic, are observed. The first endothermic starts from 50 °C and ends at 75 °C with maximum of 63 °C, giving a ΔH value of 14.00 kJ/mol, Table 7. This endothermic step is due to the evolution of water molecule. The second endothermic one involving enthalpy value ($\Delta H = 8.45$ kJ/mol). This step shows the phase transition due to partial melt of the complex. These step followed by two strong exothermic peak starting from 260 up to 313 °C with maximum of 312.4 °C involving ΔH value of −321.4 kJ/mol and the other one starting from

Table 8
Kinetic parameters for the non-isothermal decomposition of the DMT–Good's buffer complexes

Temperature range	Step	ΔE (kJ/mol)	A (s^{-1})	Ti (K)	ΔS^* (J/mol K)	ΔG^* (kJ/mol)	ΔH^* (kJ/mol)
DMT-Mes							
89–112	I	155.1	5.5E+20	375.05	150.2	98.7	152.0
319–357	II	61.9	6.1E+05	614.55	−140.3	148.1	56.8
595–610	III	−4.2	1.0E+03	853.55	−195.9	163.0	−11.3
1046–1152	IV	115.6	1.3E+03	1379.85	−197.9	388.6	104.1
DMT-Mops							
26–72	I	155.2	2.6E+23	332.45	202.3	87.9	152.4
278–296	II	369.4	5.7E+33	562.75	396.1	146.6	364.8
312–319	III	203.3	3.1E+17	592.65	84.4	153.3	198.4
385–513	IV	30.2	9.9E+00	727.05	−233.3	199.8	24.2

313 °C up to 335 °C with maximum of 335.0 °C involving ΔH value of −110.68 kJ/mol. The third and fourth endothermic peaks starts from 344 up to 658 °C with maximum of 380 °C and 649.4 °C involving ΔH value of 119.9 and 62.50 kJ/mol. These endothermic peaks are followed by an exothermic transition starting from 707.0 up to 726.0 °C with maximum of 700.7 °C which gives ΔH value of −37.05 kJ/mol Table 8.

11. Calculation of activation thermodynamic parameters of the decomposed complexes

The thermodynamic activation parameters of decomposition process of dimethyltin(IV)-Good's buffer complexes namely activation energy (E^*), enthalpy (ΔH^*), entropy (ΔS^*) and free energy of the decomposition (ΔG^*), are evaluated graphically by employing the Coats–Redfern [44,45] method using the relation:

$$\log\left[\frac{\log(W_f/W_f - W)}{T^2}\right] = \log\left[\frac{AR}{\theta E^*}(1 - \frac{2RT}{E^*})\right] - \frac{E^*}{2.303RT} \quad (5)$$

where W_f is the mass loss at the completion of the reaction, W is the mass loss up to temperature T,$R$is the gas constant, E is the activation energy in J/mol, θ is the heating rate. Since, 1–$2RT/E^* \approx 1$, a plot of the left-hand side of Eq. (5) against $1/T$ gives a slope from which E^* is calculated and A (Arrhenius constant) is determined from the intercept. The calculated values of E^*, A, ΔS^*, ΔH^* and ΔG^* for the decomposition steps are given in Table 7. According to the kinetic data obtained from DrTGA curves, all the complexes have (−ve) entropy except step III of DMT–Mes complex (estimated mass loss 3.95%, theoretical 3.98%) mass loss which indicates that activated complexes have more ordered systems than reactants.

12. Conclusion

1. The measurement and assessment of pH in the biological field is well defined and documented.
2. The formation equilibria of DMT(IV) complexes involving zwitterionic buffer (Mes and Mops) were investigated at different temperatures and variation of water–dioxane proportion.
3. In combination of stability constants data of such DMT(IV) hydrolysis complexes with zwitterionic buffer (Mes or Mops) it would be possible to calculate the equilibrium distribution of the metal species in biological fluids at different (temperature and solvent). This would form a clear basis for understanding the mode of action of such metal species under physiological conditions.
4. Thermodynamic parameters such as activation energy (E_a), pre-exponential factor (A), entropy of activation (ΔS^*) and free energy of activation (ΔG^*) have been calculated for each step, employing integral method Coats and Redfern equation.
5. The negative values of ΔS^* indicate that the activated complexes have a ordered structure than the reactants and the reactions are slower than normal.
6. Also the greater enthalpy and the lower activation energy are responsible for greater binding between ligand and dimethyltin(IV) atom in the complexes.

References

[1] C.J. Evans, in: P.J. Smith (Ed.), Chemistry of Tin, Blackie Academic and Professional, London, 1998, p. 442.
[2] S. Durand, K. Sakamoto, T. Fukuyama, A. Orita, J. Otera, A. Duthie, D. Dakternieks, M. Schulte, K. Jurkschat, Organometallics 19 (2000) 3220.
[3] D.P. Miller, P.J. Craig, in: P.J. Smith (Ed.), Chemistry of Tin, Blackie Academic and Professional, London, 1998, p. 541.
[4] I. Omae, Appl. Organometal. Chem. 17 (2003) 81.
[5] M. Gielen, Appl. Organometal. Chem. 16 (2002) 481.
[6] M. Gielen, Coord. Chem. Rev. 151 (1996) 41.
[7] J. Beckmann, K. Jurkschat, Coord. Chem. Rev. 215 (2001) 267.
[8] V. Chandrasekhar, S. Nagendran, V. Baskar, Coord. Chem. Rev. 235 (2002) 1.
[9] N.E. Good, G.D. Winget, W. Winter, T.N. Connolly, S. Izawa, R.M.M. Singh, Biochemistry 5 (1966) 467.
[10] N.E. Good, S. Izawa, Methods Enzymol. 24 (1972) 53.
[11] W.J. Ferguson, K.I. Braunschweiger, W.R. Braunschweiger, J.R. Smith, J.J. McCormick, C.C. Wasmann, N.P. Jarvis, D.H. Bell, N.E. Good, Anal. Biochem. 104 (1980) 300.
[12] J.D. Gregory, S.W. Sajdera, Science 169 (1970) 97.
[13] R. Nakon, C.R. Krishnamoorthy, Science 221 (1983) 749.
[14] J.M. Pope, P.R. Stevens, M.T. Angotti, R. Nakon, Anal. Biochem. 103 (1980) 214.
[15] Z.M. Anwar, H.A. Azab, J. Chem. Eng. Data 44 (1999) 1151.
[16] H.A. Azab, F.S. Deghaidy, A.S. Orabi, N.Y. Farid, J. Chem. Eng. Data 45 (2000) 709.
[17] Z.M. Anwar, H.A. Azab, J. Chem. Eng. Data 46 (2001) 34.
[18] E. Abd-Alla, M.M.A. Mohamed, M.R. Mahmoud, J. Coord. Chem. 56 (2003) 691.
[19] R.G. Bates, Determination of pH-Theory and Practice, second ed., Wiley, New York, 1975.
[20] M.M. Shoukry, W.M. Hosny, M.M. Khalil, Trans. Met. Chem. 20 (1995) 252.
[21] O. Al-Flaijj, M.M.A. Mohamed, M.R. Shehata, M.M. Shoukry, Monatsh. für Chem. 132 (2001) 349.
[22] P. Gans, A. Sabatini, A. Vacca, Inorg. Chem. Acta 18 (1976) 237.
[23] L. Pettit, Acad. Software (2002).
[24] P. Surdy, P. Rubini, N. Buzás, B. Henry, L. Pellerito, T. Gajda, Inorg. Chem. 38 (1999) 346.
[25] T. Natsume, S. Aizawa, K. Hatano, S. Funahshi, J. Chem. Soc., Dalton Trans. (1994) 2749.
[26] N. Buzás, T. Gajda, L. Nagy, E. Kuzmann, A. Vertes, K. Burger, Inorg. Chim. Acta 274 (1998) 167.
[27] G. Arena, R. Purrello, E. Rizzarelli, A. Gianguzza, L. Pellerito, J. Chem. Soc., Dalton Trans. (1989) 773.
[28] A.A. Al-Najjar, M.R. Shehata, M.M.A. Mohamed, M.M. Shoukry, Main Group Met. Chem. 22 (1999) 253.
[29] H.E. Mash, Y-P. Chin, L. Sigg, R. Hari, H. Xue, Anal. Chem. 75 (2003) 671.
[30] D.O. Rees, J. Mol. Biol. 141 (1980) 323.
[31] N.K. Rogers, G.R. Roore, M.J.E. Strenberg, J. Mol. Biol. 182 (1985) 613.
[32] H. Sigel, R.B. Martin, R. Tribolet, U.K. Haring, R. Malini-Balakrishran, Eur. J. Biochem. 152 (1985) 187.
[33] G. Akerlof, O.A. Short, J. Am. Chem. Soc. 75 (1953) 6357.

[34] H. Sigel, Pure Appl. Chem. 61 (1989) 923.
[35] S.A. Orabi, F.S. Deghaidy, H.A. Azab, H. Said, Synth. React. Inorg. Met.-Org. Chem. 31 (2001) 695.
[36] N. Buzás, B. Gyurcsik, L. Nagy, Y. Zhang, L. Korecz, K. Burger, Inorg. Chim. Acta 218 (1994) 65.
[37] T.P. Lockhart, W.F. Manders, J. Am. Chem. Soc. 107 (1985) 4546.
[38] T.P. Lockhart, W.F. Manders, J. Organomet. Chem. 25 (1986) 892.
[39] M. Honda, M. Komura, Y. Kawasaki, T. Tanaka, R. Okawara, J. Inorg. Nucl. Chem. 30 (1968) 3231.
[40] Y. Maeda, C.R. Dillard, R. Okawara, Inorg. Nucl. Chem. Lett. 2 (1966) 197.
[41] Ramão M. Fernandes, Ernesto S. Lang a, Ezequiel M.V. López, Gerimário F. de Sousa, Polyhedron 21 (2002) 1149.
[42] J.W. Dodd, K.H. Tonge, "Thermal methods" Analytical Chemistry by Open Learning, Wiley, New York, 1987, p. 117.
[43] K. Nagase, Bull. Chem. Soc. Jpn. 45 (1972) 2166.
[44] A. Coats, J. Redfern, Nature 201 (1964) 68.
[45] D.W. Johnson JR, P.K. Gallagher, J. Phys. Chem. 76 (1972) 1474.